Selecting Parameters for GMAW Using Dimensional Analysis

Regression and dimensional analysis of experimental data established relationships between welding parameters and process variables

BY P. E. MURRAY

ABSTRACT. A method for analyzing gas metal arc welding procedures was developed to select welding parameters that lead to a desired operating condition. Analytical relationships between welding parameters and process variables were established by regression and dimensional analysis of experimental data. This data was obtained from a detailed GMA welding experiment in which the welding parameters were precisely controlled and the process variables precisely measured and correlated. Using nondimensional variables to correlate experimental data, accurate analytical relationships between welding parameters, arc process variables, and bead geometry were obtained. The analytical relationships for bead geometry extended the work of previous researchers by introducing a nondimensional mass transfer number and demonstrating the dependence of bead geometry on mass transfer as well as heat transfer. These relationships were used to identify a range of stable welding parameters and to find the welding parameters needed to ensure process constraints were met. Specific welding parameters were found by controlling arc length and weld bead geometry to ensure arc stability, adequate weld bead size, and adequate joint penetration.

Introduction

Selecting an optimal welding procedure is important because optimal procedures ensure weld quality and reliability of the welding process while enhancing productivity through elimination of rework. Currently, selecting the welding process, choosing the welding consumables, and optimizing the welding parameters are independent tasks. Furthermore, welding procedures are often developed with handbooks and manufacturers' recommendations based on a large amount of empirical data, and welding parameters are often found by trial and error. Consequently, the welding procedure may not be optimal regarding weld quality and productivity.

A weld must meet acceptance criteria that stem from the need to ensure weld quality and mechanical integrity. Reducing the occurrence of weld defects and distortion, and enhancing the mechanical properties of the weld are some considerations in selecting a welding procedure that meets acceptance criteria. These criteria often limit the welding procedure regarding heat input, joint design, welding technique, and composition of welding consumables. However, variability in weld quality is inherent due to operator error, contamination of the welded parts, and disturbances caused by variations in joint geometry and position of the arc welding gun. Monitoring and controlling weld variability and eliminating defects has been an elusive goal. Therefore, a method for selecting an optimal welding procedure is needed to improve weld quality and to increase the likelihood that each weld meets acceptance criteria.

Analysis has been used to establish relationships between welding parameters, weld bead geometry, weld quality, and productivity, and to select welding parameters leading to an optimal process. An early paper on this subject is found in Ref. 1. Research to find more accurate and efficient methods for selecting welding parameters is ongoing, and several notable examples are found in Refs. 2–11. These methods include optimization (Refs. 2, 3), neural networks (Refs. 4, 5), and regression (Refs. 6–9); a related approach that is entirely empirical is described in Ref. 10. In fact, selecting optimal welding parameters is often based on analytical and empirical methods that are computationally efficient. However, analytical methods have deficiencies stemming from simplifying assumptions, and empirical methods are valid only for the processes and consumables used to obtain the experimental data. Nonetheless, analytical and empirical methods are often used to select optimal welding parameters because the complexity of the weld process usually precludes detailed numerical simulation. Recently, an efficient numerical approach was used to simulate thermal phenomena that occur during welding, and to optimize welding parameters for controlling weld bead geometry (Ref. 11).

In this study, a method was developed for analyzing gas metal arc welding procedures to select welding parameters for a desired operating condition. A welding parameter is directly controlled by the welder, for example a machine setting, whereas a process variable depends on welding parameters and is controlled indirectly by the welder. Welding parameters in constant voltage GMAW include open circuit voltage, travel speed, wire feed speed, wire diameter, and contact tube-to-work distance. Process variables pertaining to the welding arc include current, melting rate, arc length, arc voltage, and arc resistance; process variables pertaining to weld geometry include bead depth, bead width, bead area, and deposited metal area. Generally, welding parameters are chosen to satisfy process constraints stemming from the need to reduce the occurrence of weld defects. In this study, welding parameters were found by constraining process variables to obtain desired arc attributes and

KEY WORDS

Gas Metal Arc
GMAW
Arc Length
Bead Geometry
Process Variables
Welding Parameters

P. E. MURRAY is with Bechtel BWXT Idaho, LLC, Idaho National Engineering and Environmental Laboratory, Idaho Falls, Idaho.

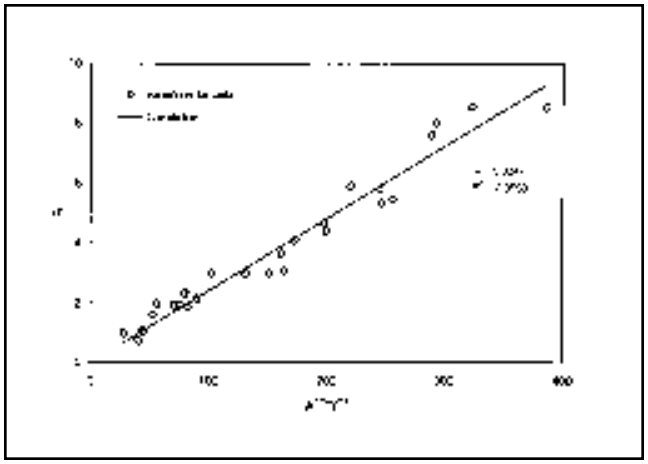

Fig. 1 — Correlation between the nondimensional depth of fusion, mass transfer number, and heat transfer number.

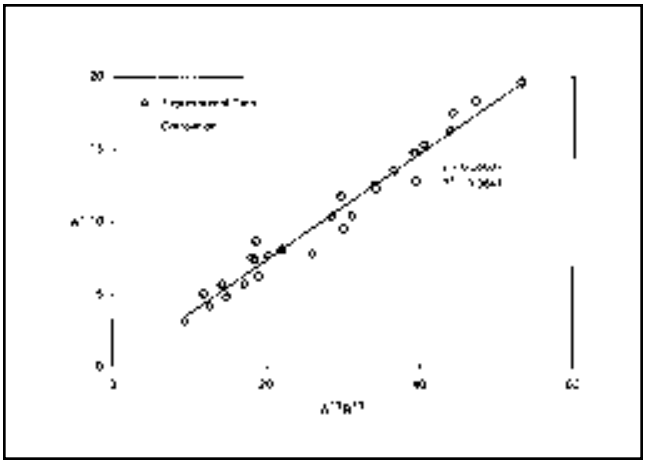

Fig. 2 — Correlation between the nondimensional weld bead width, mass transfer number, and heat transfer number.

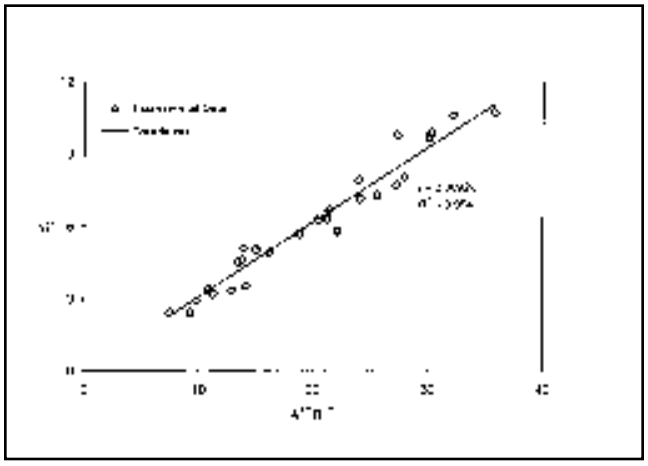

Fig. 3 — Correlation between the nondimensional weld bead area, mass transfer number, and heat transfer number.

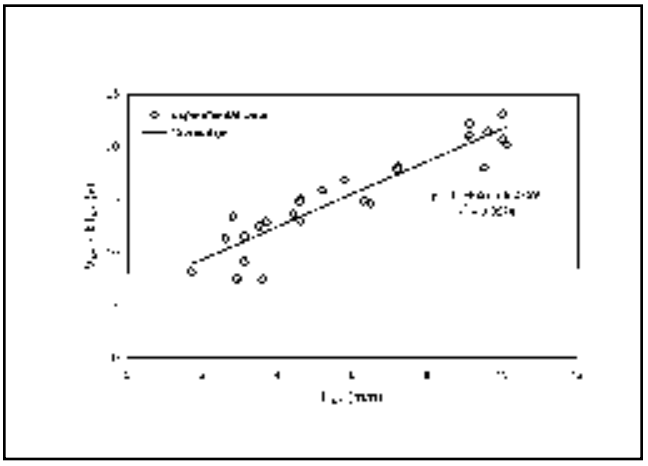

Fig. 4 — Correlation between arc length, arc voltage, and current.

weld bead geometry.

The method for selecting welding parameters included experimentation and analysis as described below. First, experimental data for a range of operating conditions was obtained from a detailed GMA welding experiment in which the welding parameters were precisely controlled and the process variables precisely measured. Accurate analytical relationships between welding parameters and process variables were established by regression and dimensional analysis of experimental data. The analytical relationships for bead geometry extended the work of previous researchers by introducing a nondimensional mass transfer number and demonstrating the dependence of bead geometry on mass transfer as well as heat transfer. Then, specific objectives were determined in regard to the process variables. These objectives included limits on arc length and desired mode of metal transfer. Other objectives related to weld bead geometry included desired values of weld bead area, joint penetration, bead width, and deposited metal area. Finally, the analytical relationships between welding parameters and process variables were used to select welding parameters needed to ensure process objectives were met.

The method for selecting welding parameters was demonstrated by an example in which specific welding parameters were found by controlling arc length, deposited metal area, and depth of fusion to ensure arc stability, adequate weld bead size, and adequate joint penetration.

The main contribution of this study is twofold: 1) dimensional analysis of experimental data to obtain analytical relationships between welding parameters and process variables; 2) a method for selecting welding parameters to obtain a desired weld bead geometry.

Experiment

Horizontal bead-on-plate welds were made on ¼- and ½-in.-thick stainless steel type ASTM 304 using an automated gas metal arc welding apparatus. A Miller Maxtron 450 power supply was used in the constant voltage mode. The shielding gas was a mixture consisting of 98% Ar_2 and 2% O_2, and the flow rate was fixed at 35 ft^3/h. The electrodes were stainless steel type AWS ER308L with diameters equal to 0.89 and 1.14 mm. An experiment was designed to vary voltage, current, electrode diameter, electrode speed, travel speed, and contact tube-to-work distance, and to determine the effect of welding parameters on arc length, weld bead geometry, and mode of mass transfer. The data obtained from this experiment is shown in Table 1.

Twenty-seven separate welds were made to produce a variation in voltage

Table 1 — Experimental Data for Gas Metal Arc Welding of Stainless Steel Using a Bead-on-Plate Weld and Shielding Gas Consisting of 98% Argon and 2% Oxygen

Electrode Diameter (mm)	Travel Speed (mm/s)	Electrode Speed (mm/s)	Arc Voltage (v)	Current (A)	Contact Tube-to-Work Distance (mm)	Arc Length (mm)	Mode of Metal Transfer	Depth of Fusion (mm)	Bead Width (mm)	Bead Area (mm^2)
1.143	7	102.3	17.6	188.8	13	1.7	Shorting	2.1	8.1	23.7
1.143	7	102.3	21.6	173.6	13	2.8	Shorting	2.5	9.3	29.8
1.143	10	146.2	26.6	255	16	4.4	Spray	3.5	9.3	35.3
0.889	10	241.7	31.1	213.3	19	9.5	Spray	3.3	9.2	28.9
0.889	10	241.7	31.3	276.3	13	9.1	Spray	4.1	11.5	36.4
0.889	7	169.2	23.5	143	16	3.7	Mixed	2.5	7.9	24.8
0.889	7	169.2	26.3	155.2	16	5.2	Spray	3.2	8.6	28.1
0.889	4	96.7	17.6	96	13	3.1	Shorting	1.9	5.8	21.0
1.143	4	58.5	28.1	128.5	19	9.1	Mixed	1.4	9.5	20.9
1.143	4	76.7	27.5	167.2	16	9.1	Mixed	3.6	10.7	39.9
0.889	7	222	25.2	216.1	13	4.6	Mixed	3.2	8.3	37.40
0.889	7	222	30.9	235.1	16	10.1	Spray	4.4	11.1	39.0
1.143	7	134.3	19.8	196.5	19	2.9	Shorting	2.3	8.2	29.3
1.143	7	134.3	28.7	244.9	16	7.2	Spray	3.9	12.6	45.9
0.889	10	317.2	24.6	197.1	19	3.6	Mixed	2.3	7.1	25.1
1.143	10	191.9	28.9	328.1	13	4.6	Spray	5.7	12.2	52.6
1.143	10	191.9	28.9	334.1	13	4.6	Spray	6.0	13.1	55.0
0.889	4	126.9	24.1	141.6	13	5.8	Mixed	3.7	9.0	36.4
0.889	7	274.5	30.2	208.8	19	6.5	Spray	3.2	11.0	45.0
1.143	4	95	21.4	168.3	16	3.5	Shorting	3.0	10.7	41.6
1.143	4	95	27	178.7	19	7.2	Spray	3.5	11.7	44.2
0.889	10	392.7	31.3	333.5	13	6.3	Spray	6.4	13.7	63.2
0.889	10	392.7	35	389.6	13	9.6	Spray	6.4	14.7	64.8
1.143	7	166.3	29.6	319.6	13	10.0	Spray	6.3	14.5	61.1
1.143	7	166.3	32.7	346.3	13	10.0	Spray	6.2	15.8	68.3
0.889	4	157.1	19.2	132.4	16	3.1	Shorting	2.0	7.8	30.3
1.143	10	237.6	28.8	315.9	16	2.6	Mixed	4.0	9.5	54.0

from 17 to 35 V and a variation in current from 90 to 390 A, which encompassed many different operating conditions. The arc was photographed using a high-speed camera designed for use with a high-intensity light source. The mode of metal transfer and the arc length were recorded for each weld. The observed mode of transfer was either short circuiting or spray. If the transfer was short circuiting with intermittent spray, the mode was called mixed. The arc length of short circuiting transfer is the maximum arc length that occurs during the nonshorting period. The metallographic samples were prepared by electrochemical etching and examined using a microscope. Magnified photographs were obtained and the weld bead geometry was measured. These measurements include depth of fusion, bead width, and bead area.

Depth is defined as the distance from the original surface of the base metal to the bottom of the zone of fused metal. Therefore, the height of the weld bead was not included in the measured depth. Two samples were prepared for each experimental condition, and the difference in weld bead size between samples was determined. This produced a distribution of differences in measured bead size, and the average uncertainty in the measurement was defined as the mean of the distribution. An estimate of the mean indicated the average uncertainty in the measurement was equal to 0.5 mm.

Analytical Relationships

Analytical relationships between welding parameters and process variables are needed for selecting weld parameters. Consider a gas metal arc welding process that is described by the data shown in Table 1. The methods of regression and dimensional analysis are used to correlate experimental data and to establish analytical relationships that are computationally efficient. Although these relationships are valid for a specific weld process, joint design, and welding consumable, the method for obtaining these relationships is generally applicable to gas metal arc welding processes.

The relationships between welding parameters and weld bead geometry are needed to determine welding parameters that lead to a desired weld bead size. Deposited metal area, weld bead area, bead width, and depth of fusion are quantities of particular interest. The deposited metal area A_d is equal to $M/\rho S$, where M is the electrode melting rate, ρ is the electrode density, and S is the travel speed. However, the effect of welding parameters on weld bead area, bead width, and depth of fusion is complex. Therefore, analytical relationships are obtained by correlating experimental data. Two nondimensional variables are introduced in order to establish a correlation. The mass transfer number is

$$A = \frac{M}{\mu r_e} \tag{1}$$

where A is the mass transfer number, μ is the viscosity of the liquid metal in the weld pool, and r_e is the radius of the electrode. The heat transfer number is

$$B = \frac{V_{arc} IS}{\Delta H \alpha^2} \tag{2}$$

where B is the heat transfer number, V_{arc} is the arc voltage, I is the current, ΔH is the change in enthalpy of the base metal heated from the initial temperature to the melting temperature, and α is the thermal diffusivity of the base metal. The nondimensional mass transfer number given by Equation 1 was introduced in Ref. 12 and represents the ratio of two time scales: the time scale associated with mass transfer from the electrode and the time scale associated with mass transfer in the weld pool. The nondimensional heat transfer number given by Equation 2 was introduced in Ref. 13 and represents the ratio of two time scales: the time scale

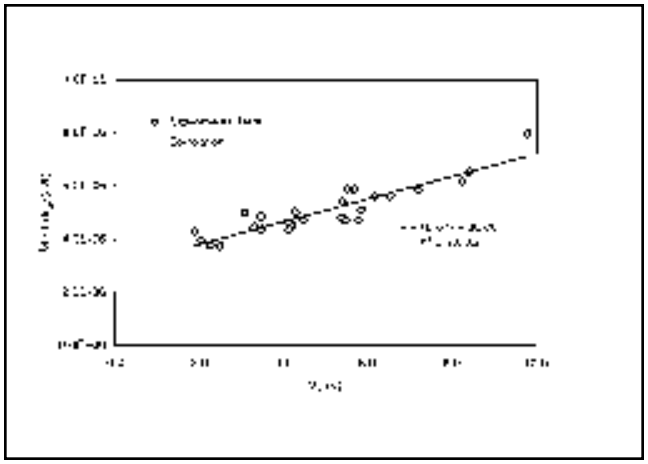

Fig. 5 — Correlation between melting rate, current, and voltage drop across the electrode extension.

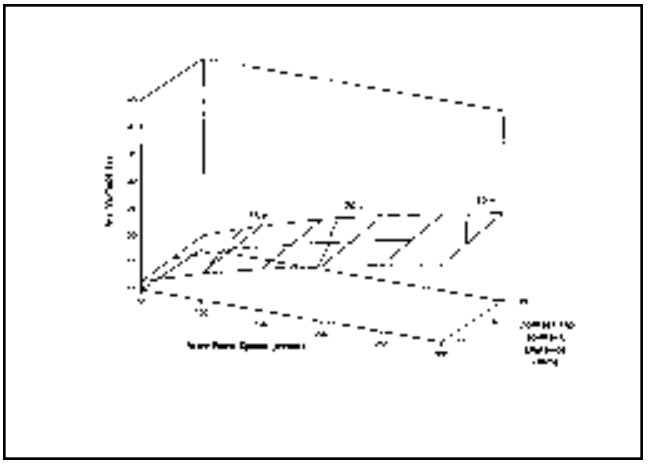

Fig. 6 — Short arc limit (zero arc length).

associated with heat transfer from the welding arc and the time scale associated with heat transfer in the weld pool.

The correlation between the depth of fusion and welding parameters is shown in Fig. 1 and is given by the following nondimensional relation:

$$\frac{d}{\alpha / S} = \eta_1 A^{1/3} B^{2/3} \qquad (3)$$

where d is the depth of fusion and η_1 is a coefficient determined empirically. Linear regression was used to find that η_1 = 0.024, with a correlation coefficient equal to 0.95. A complete description of the mathematical basis of this correlation is found in Ref. 12.

The correlation between welding parameters and weld bead width is shown in Fig. 2 and is given by the following nondimensional relation:

$$\frac{w}{\alpha / S} = \eta_2 A^{2/9} B^{4/9} \qquad (4)$$

where w is the width of the weld bead and η_2 is a coefficient determined empirically. Linear regression was used to find that η_2 = 0.37, with a correlation coefficient equal to 0.96. Similarly, the correlation between welding parameters and weld bead area is shown in Fig. 3 and is given by the following nondimensional relation:

$$\frac{\Omega^{1/2}}{\alpha / S} = \eta_3 A^{1/5} B^{2/5} \qquad (5)$$

where Ω is the area of the weld bead and η_3 is a coefficient determined empirically. Linear regression was used to find that η_3 = 0.31, with a correlation coefficient equal to 0.95. The relationships given by Equations 3–5 and the method for selecting welding parameters to obtain a desired weld bead size are the main contributions of this study.

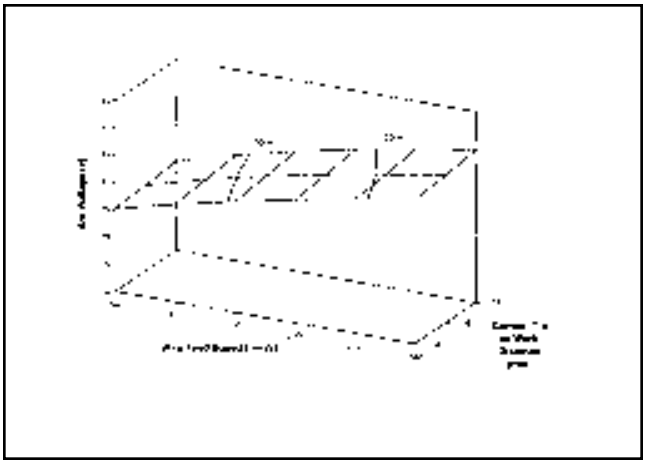

Fig. 7 — Long arc limit (10-mm arc length).

A noteworthy observation is that Equations 3–5 suggest a general correlation between the nondimensional depth, width, area, and the nondimensional variable AB^2. This result underscores the importance of using dimensional analysis to simplify correlation of experimental data and to reduce the number of regression coefficients. In fact, each correlation has only two regression coefficients that are easily found by least squares.

The dependence of weld bead geometry on the heat transfer number B was described analytically by Christensen, *et al.* (Ref. 13). In this study, dimensional analysis of the welding process was extended to include the dependence of bead geometry on the mass transfer number A. The physical basis for this correlation is the effect of mass transfer on bead shape, which was observed experimentally by Essers and Walter (Ref. 14). In particular, the experiments presented in Ref. 14 suggest bead depth is affected by the mass and momentum of droplets impinging the weld pool, which supports this study's finding that bead geometry depends on the mass transfer number A. Linear regression was used to ascertain a simple and fitting relationship between bead geometry and the nondimensional variables A and B. Using data on the variation of bead size with respect to A and B, an accurate correlation between bead geometry and the nondimensional variable AB^2 was established. A detailed discussion of the mathematical and statistical basis for this correlation is given in Ref. 12.

Additional relationships between voltage, current, arc length, melting rate, and electrode extension are needed to determine welding parameters that lead to a stable operating condition. Simple, steady-state relationships are suitable for this purpose. These relationships are auxiliary since Equations 1–5 and the

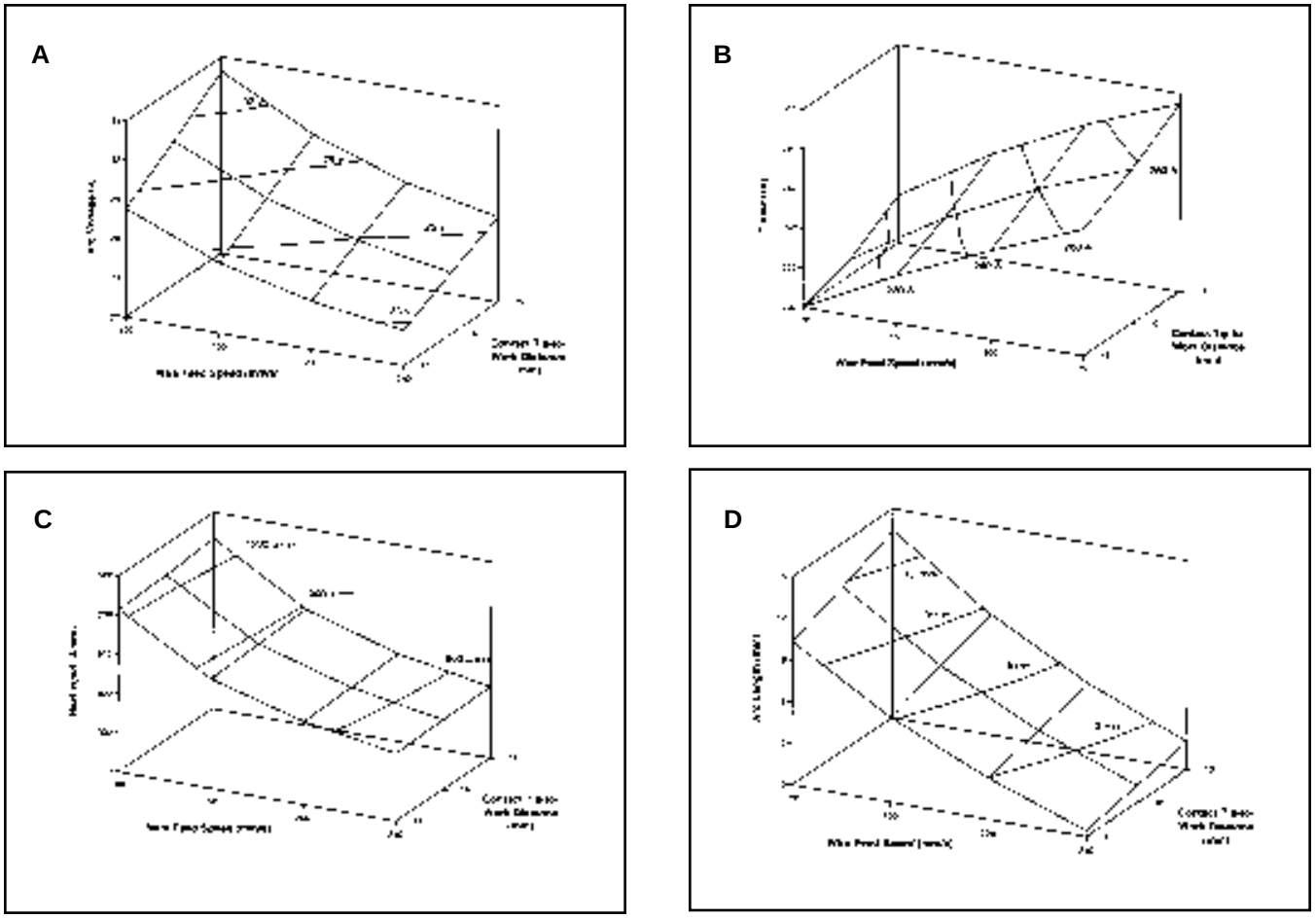

Fig. 8 — Operating points needed to obtain depth of fusion = 4 mm and deposited metal area = 25 mm². A — Arc voltage, wire feed speed, and contact tube-to-work distance; B — current, wire feed speed, and contact tube-to-work distance; C — heat input, wire feed speed, and contact tube-to-work distance; D — arc length, wire feed speed, and contact tube-to-work distance.

method of selecting welding parameters comprise the main contributions of this paper. The correlation between voltage, current, and arc length is shown in Fig. 4, and is given by the following equation

$$V_{arc} = IR_{arc} + a_0 + a_1 L_{arc} \quad (6)$$

where V_{arc} is the arc voltage, I is the current, R_{arc} is the arc resistance, L_{arc} is the arc length, a_0 is the anode and cathode voltage drops, and a_1 is the arc potential gradient. This correlation is described in Ref. 15, where it was found that R_{arc} = 0.020 ohms for the shielding gas used in this study. Linear regression was used to find that a_0 = 6.3 v and a_1 = 1.55 v/mm, with a correlation coefficient equal to 0.86. The correlation between melting rate, current, and electrode extension is shown in Fig. 5, and is given by the equation:

$$M = b_0 I + b_1 V_e I \quad (7)$$

where M is the electrode melting rate, b_0 is the anode heating coefficient, b_1 is the joule heating coefficient, and V_e is the voltage drop across the electrode extension. This correlation is described in Ref. 16. In the case of a cylindrical electrode

$$M = \rho U A_e \quad (8)$$

$$V_e = \frac{\sigma L_e I}{A_e} \quad (9)$$

where ρ is the electrode density, σ is the electrode resistivity, L_e is the electrode extension into the arc, A_e is the electrode cross-sectional area, and U is the speed of the electrode that is fed into the arc. The variable U is called the wire feed speed, and the sum of L_{arc} and L_e is called the contact tube-to-work distance. For the electrode used in this study, ρ = $8 \cdot 10^{-3}$ g/mm³ and σ = $2.7 \cdot 10^{-3}$Ω–mm. The resistivity used in Equation 9 is the mean value of the resistivities at room temperature and melting temperature. Linear regression was used to find that b_0 = $3 \cdot 10^{-6}$kg/s–A and b_1 = $4 \cdot 10^{-7}$kg/s–A–v, with a correlation coefficient equal to 0.82. Finally, the power supply characteristic curve is given by the following relation:

$$V_{oc} = V_{arc} + \gamma I \quad (10)$$

where V_{oc} is the open circuit voltage, and γ is the power supply slope that is equal to 0.03 v/A for the power supply used in this study. Equations 6–10 are used to compute the mean values of arc voltage, current, arc length, and electrode extension, using the open circuit voltage, electrode diameter, and wire feed speed as inputs. In this manner, the limiting conditions of short and long arc length may be identified.

Note that Equations 6–10 describe the mean values of voltage, current, and arc length. The instantaneous values of these variables are affected by the dynamics of the power supply, which causes oscillations in voltage, current, and arc length.

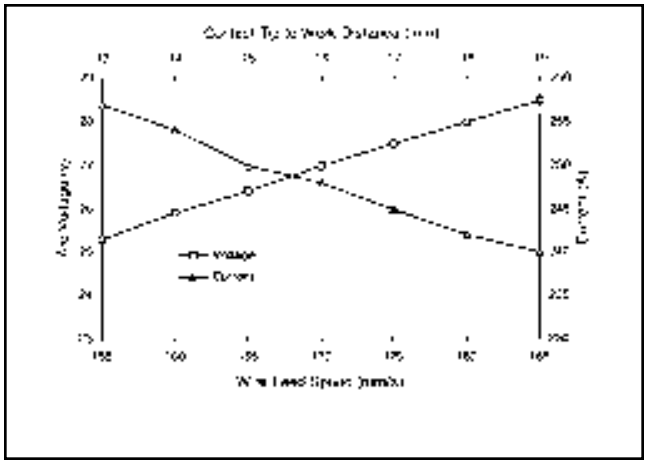

Fig. 9 — Operating points needed to obtain depth of fusion = 4 mm, deposited metal area = 25 mm², and arc length = 6 mm.

However, these oscillations occur at a time scale that is much smaller than the time scale associated with melting and solidification of the weld bead. Therefore, the steady-state relationships given by Equations 6–10 are suitable for determining the effect of electrical parameters on weld bead geometry.

Method

Generally, the method for selecting welding parameters includes the following steps:

1) Study the process experimentally for a range of welding parameters to gather data on the process variables pertaining to the arc and weld bead. For example, the data shown in Table 1 forms a sample large enough to establish accurate analytical relationships. Use the methods of regression and dimensional analysis to correlate experimental data and to establish the analytical relationships given by Equations 1–10. In this study, the data was entered into a spreadsheet, the nondimensional variables were computed, the results were graphed, and regression was used to obtain accurate analytical relationships. Then, a computer program was developed to evaluate the resulting equations and to compute the process variables for any given set of welding parameters. The desired parameters were found by computing solutions to the equations for a range of parameters and graphing the results to find the parameters that lead to specific values of the process variables.

2) Analyze the process to find specific values of arc voltage, wire feed speed, and contact tube-to-work distance that lead to a stable arc. In particular, compute the short arc limit and the long arc limit to identify a range of stable welding parameters. The operating range is described by a region in (V_{arc}, U, L) parameter space, where V_{arc} denotes arc voltage, U denotes wire feed speed, and L denotes contact tube-to-work distance. In this case, a specific operating point in (V_{arc}, U, L) parameter space subject to a constraint on the arc length fixes the open circuit voltage.

3) Select a desired value of deposited metal area. This objective implies that the ratio of wire feed speed to travel speed is constant for a fixed electrode diameter.

4) Select a desired value of depth of fusion, weld bead width, or weld bead area. Analyze the process to find specific values of arc voltage, wire feed speed, and contact tube-to-work distance that lead to the desired weld bead geometry. The operating range of these parameters is described by a surface in (U, L) parameter space.

5) Select a desired mode of metal transfer and a desired arc length. Analyze the process to find specific values of arc voltage, wire feed speed, and contact tube-to-work distance that lead to the desired arc length. Compare the computed current and the measured transition current to verify the desired mode of metal transfer is obtained. The operating range is reduced to a line that depends on a single parameter, U or L. Finally, particular welding parameters may be selected empirically from the reduced set of operating points.

Example and Discussion

In this section, the method is demonstrated by selecting parameters for welding stainless steel, using the experimental data shown in Table 1 and the relationships given by Equations 1–10. In the following discussion, an electrode diameter equal to 1.2 mm is assumed. First, consider the problem of computing the welding parameters that lead to a stable arc. The computed short arc limit for L_{arc} = 0 mm is shown in Fig. 6, and the computed long arc limit for L_{arc} = 10 mm is shown in Fig. 7. These limiting conditions determine the range of arc voltage, wire feed speed, and contact tube-to-work distance needed to sustain a stable arc. These results may be used to select welding parameters that lead to a desired arc length. Next, consider the problem of computing the welding parameters that lead to desired values of deposited metal area and depth of fusion to ensure bead size and joint penetration are adequate. Suppose the desired deposited metal area is equal to 25 mm² and the desired depth of fusion is equal to 4 mm. The operating conditions needed to obtain these desired objectives are computed and shown in Fig. 8. These results identify a range of voltage, wire feed speed, contact tube-to-work distance, and the effect on current, heat input (V_{arc}I/S), and arc length. Since deposited metal area and electrode diameter are fixed, the travel speed is proportional to the wire feed speed.

To select a particular operating condition, additional objectives and constraints are identified. For example, suppose spray transfer is desired; in this case, the minimum current for spray transfer is equal to 225 A. Furthermore, a lower limit on the arc length is needed to avoid short circuiting and to ensure arc stability in spray transfer. Suppose an arc length equal to 6 mm is desired. The results shown in Fig. 8 may be used to select specific values of arc voltage, wire feed speed, and contact tube-to-work distance that lead to this particular arc length while maintaining desired values of deposited metal area and depth of fusion. These operating points and the effect on current are shown in Fig. 9. Furthermore, spray transfer is obtained at each operating point because the current exceeds the minimum current for spray transfer.

The set of welding parameters illustrated in Figs. 6–9 is obtained by solving Equations 1–10 augmented by process constraints on weld bead geometry and arc length. In this example, an operating point is given by specific values of arc voltage, current, wire feed speed, and contact tube-to-work distance that lead to deposited metal area equal to 25 mm², depth of fusion equal to 4 mm, and arc length equal to 6 mm. Generally, the analytical method developed in this study may be used to obtain a set of welding parameters leading to specific objectives that may be different than those used here.

Equations 1–10 augmented by specific constraints must be solved to obtain a reduced set of operating points or a unique operating point satisfying specific objectives determined by the requirements of the weld procedure. For example, a constraint on bead depth may be replaced by a constraint on bead width. Applying simultaneous constraints on bead depth and bead width may overconstrain the equations and, in this case, it may be necessary to relax the constraints on arc

length or deposited metal area to obtain a solution. Numerous combinations of constraints that lead to a solution may be found. In each case, Equations 1–10 are the starting point for dimensional analysis of the weld process. Furthermore, the accuracy of the analytical relationships has been demonstrated in the case of a specific weld process, base metal, consumable, joint design, and welding technique. The analysis may be extended to include other materials, but the accuracy of the correlation may be sensitive to variations in the properties of the base metal.

Summary

A method was developed for analyzing gas metal arc welding procedures to select welding parameters that lead to desired operating conditions. Analytical relationships were used to identify a range of stable welding parameters and to find the welding parameters needed to ensure process constraints are met. Specific welding parameters were found by controlling arc length, depth of fusion, and deposited metal area, leading to arc stability, adequate weld bead size, and adequate joint penetration. The method may be used to select welding parameters for controlling other process variables that affect weld quality, including bead area and bead width. In this manner, dimensional analysis may be used to analytically describe the complex relationships between welding parameters, arc process variables, and bead geometry, in order to find a set of suitable welding parameters without the need to perform a multitude of welding experiments.

Furthermore, the accuracy of the analytical relationships has been demonstrated in the case of a specific weld process, base metal, consumable, joint design, and welding technique. Additional research is needed to evaluate the method for application to other welding procedures.

Acknowledgments

This work was supported by the U.S. Department of Energy, Office of Science, Office of Basic Energy Sciences, under DOE Idaho Operations Office Contract DE-AC07-99ID13727. The author is grateful to Prof. A. Scotti at the Universidade Federal De Uberlandia in Brazil, for assistance in the experimental work.

References

1. Salter, G. R., and Doherty, J. 1981. Procedure selection for arc welding. *Metal Construction* 13(9): 544–550.

2. Mitchiner, J. L., Kleban, S. D., Hess, B. V., Mahin, K. W., and Messink, D. 1995. SmartWeld: A Knowledge-Based Approach to Welding. Technical Report SAND-96-1372C.

3. Eisler, G. R., and Fuerschbach, P. W. 1997. SOAR: An extensible suite of codes for weld analysis and optimal weld schedules. *Proc. 7th Intl. Conf. on Computer Technology in Welding,* ed. T. A. Siewert, pp. 257–268. San Francisco, Calif., NIST.

4. White, D., and Jones, J. 1997. Process modeling with neural networks for pulsed GMAW braze welds. *JOM* 49(9): 49–53.

5. Chan, B., Pacey, J., and Bibby, M. 1999. Modelling gas metal arc weld geometry using artificial neural network technology. *Can. Metall. Quart.* 38(1): 43–51.

6. Jackson, C. E., and Shrubsall, A. E. 1953. Control of penetration and melting rate with welding technique. *Welding Journal* 32: 172-s to 178-s.

7. Kim, I. S., Kwon, W. H., and Siores, E. 1996. An investigation of a mathematical model for predicting weld bead geometry. *Can. Metall. Quart.* 35(4): 385–392.

8. Kim, I. S., Basu, A., and Siores, E. 1996. Mathematical models for control of weld bead penetration in the GMAW process. *Int. J. Adv. Manuf. Technol.* 12: 393–401.

9. Murray, P. E. 1999. A method for optimizing welding processes. *Proc. 9th Intl. Conf. on Computer Technology in Welding,* Detroit, Mich., ed. T. A. Siewert, pp. 452–461. American Welding Society, Miami, Fla.

10. Harwig, D. D. 1997. The *ARCWISE* technique for increasing productivity in arc welding. *International Conference on Advances in Welding Technology*, Columbus, Ohio.

11. Dilthey, U., Roosen, S., and Sudnik, V. 1997. *MAGSIM* and *SPOTSIM*: PC aided simulation of GMA and spot welding processes. *Proc. 7th Intl. Conf. on Computer Technology in Welding,* ed. T. A. Siewert, pp. 548–561, San Francisco, Calif., NIST.

12. Murray, P. E., and Scotti, A. 1999. Depth of penetration in gas metal arc welding. *Science and Technology of Welding and Joining* 4(2): 112–117.

13. Christensen, N., Davies, V. de L., and Gjermundsen, K. 1965. Distribution of temperatures in arc welding. *British Welding Journal* 2: 54–75.

14. Essers, W. G., and Walter, R. 1981. Heat transfer and penetration mechanisms with GMA and plasma-GMA welding. *Welding Journal* 60: 37-s to 42-s.

15. Shepard, M. E., and Cook, G. E. 1992. A nonlinear time-domain simulation of self-regulation in gas metal arc welding. *Proc. 3rd Intl. Conf. on Trends in Welding Research*, Gatlinburg, Tenn. eds. S. A. David, and J. M. Vitek, pp. 905–910. ASM International, Materials Park, Ohio.

16. Lesnewich, A. 1958. Control of melting rate and metal transfer in gas shielded metal arc welding: control of electrode melting rate. *Welding Journal* 37: 343-s to 353-s.

Nomenclature

$A = M/\mu r_e$	nondimensional mass transer number
A_d	deposited metal area (mm^2)
A_e	electrode cross-sectional area (mm^2)
a_0	anode and cathode voltage drop (v)
a_1	arc potential gradient (v/mm)
$B = V_{arc}IS/\Delta H\alpha^2$	nondimensional heat transfer number
b_0	anode heating coefficient (kg/s-A)
b_1	joule heating coefficient (kg/s-A-v)
d	depth of fusion (mm)
$d^* = dS/\alpha$	nondimensional depth of fusion
I	current (A)
L_{arc}	arc length (mm)
L_e	electrode extension (mm)
M	electrode melting rate (kg/s)
R_{arc}	arc resistance (ohms)
r_e	electrode radius (mm)
S	travel speed (mm/s)
U	wire feed speed (mm/s)
V_{arc}	arc voltage (v)
V_e	electrode extension voltage drop (v)
V_{oc}	open circuit voltage (v)
w	weld bead width (mm)
$w^* = wS/\alpha$	nondimensional weld bead width
α	thermal diffusivity (mm^2/s)
ΔH	change in enthalpy (J/mm^3)
γ	power supply slope (v/A)
η_1,η_2,η_3	nondimensional regression coefficients
μ	viscosity (kg/mm-s)
ρ	electrode density (kg/mm^3)
σ	electrode resistivity (ohm-mm)
Ω	weld bead area (mm^2)
$\Omega^* = \sqrt{\Omega S/\alpha}$	nondimensional weld bead area